EXPERIMENTAL STUDIES OF DIFFRACTIVE PROCESSES AT HERA

A.A. SAVIN
ON BEHALF OF THE H1 AND ZEUS COLLABORATIONS
University of Wisconsin,1150 University Ave.,Madison WI 53706-1390, USA
E-mail: savin@mail.desy.de

Diffractive processes in photon-proton interactions at HERA offer the opportunity to improve the understanding of the transition between the soft, non-perturbative regime in hadronic interactions at $Q^2 = 0$ and the perturbative region at high Q^2. Recent experimental results from HERA on inclusive diffractive scattering, exclusive vector meson production and the properties of the hadronic final state in diffraction are reviewed. The results are discussed in the context of current theoretical models.

1 Introduction

One of the most important results from the ep collider HERA is the observation that about 10% of deep inelastic scattering (DIS) events exhibit a large rapidity gap between the direction of the proton beam and that of the first significant deposition in the detector, thus showing a behaviour typical for diffractive interactions[1,2]. These events could be interpreted in terms of the exchange of a colour-singlet object known as the Pomeron ($I\!P$), that can be described in QCD-inspired models as an object whose partonic composition is dominated by gluons. Alternatively, the diffractive process can be described

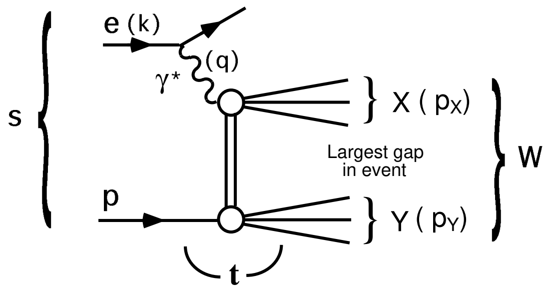

Figure 1. A generic diffractive process at HERA.

by the dissociation of the virtual photon into a $q\bar{q}$ or $q\bar{q}g$ final state that interacts with the proton by exchange of a gluon ladder [3].

Figure 1 illustrates the generic diffractive process at HERA of the type $ep \to eXY$. The positron couples to a virtual photon $\gamma^*(q)$ which interacts with the proton (P). Together with the usual kinematic variables like Q^2, y, W and x, one uses t, for the 4-momentum transferred at the proton vertex, M_X and M_Y for the invariant masses of the photon and proton dissociative systems, respectively. $x_{I\!P} = \frac{q\cdot(P-P_Y)}{q\cdot P}$ is the fraction of proton momentum carried by the $I\!P$ and $\beta = \frac{x}{x_{I\!P}}$ is the fraction of the $I\!P$ momentum carried by parton coupling to γ^*.

The main HERA results can be divided into two parts: inclusive diffraction, such as $F_2^{D(3)}$, jets and hadronic final state studies and exclusive diffraction, mainly the vector meson measurements.

2 Results

2.1 Inclusive diffraction

A high precision inclusive measurement of $F_2^{D(3)}(\beta, Q^2, x_{I\!P})$ was performed recently by H1 in the kinematic range $6.5 < Q^2 < 120$ GeV^2, $0.01 < \beta < 0.9$ and $10^{-4} < x_{I\!P} < 0.05$. The $x_{I\!P}$ dependence of the data was interpreted in terms of a measurement of the effective pomeron intercept $\alpha_{I\!P}(0)$ that was found to be

$\alpha_{I\!P}(0) = 1.173 \pm 0.018(stat.) \pm 0.017(syst.)^{+0.063}_{-0.035}(model)$.

Two further fits were performed in order to investigate whether $\alpha_{I\!P}(0)$ has any dependence on Q^2, the results are shown in Fig. 2. The values are significantly higher than the value $\alpha_{I\!P}(0) = 1.08$ for the *soft pomeron* [5], but apparently lower than for inclusive $F_2(x, Q^2)$ measurements.

At fixed $x_{I\!P}$, a flat β and a rising Q^2 dependencies were observed. This structure was well described by a fit based on DGLAP evolution with diffractive parton distributions of the proton heavly dominated by a large gluon density. This observation is in good agreement with the previous $F_2^{D(3)}$ measurements [6].

Recently ZEUS updated the diffractive cross section measurement at very low Q^2. The cross sections for different W and M_X values as a function of Q^2 are compared with the predictions of the saturation dipole-model [7] in Fig. 3. The continuous curves indicate the model predictions for $q\bar{q}+q\bar{q}g$ fluctuations, the dashed ones are the predictions if only $q\bar{q}$ fluctuations are considered. It is obvious that the $q\bar{q}$ configuration alone does not describe the data.

A measurement of dijet cross sections yields direct constrain on the diffrac-

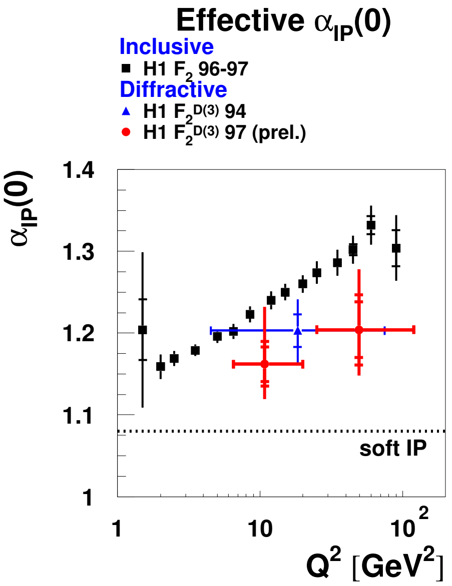

Figure 2. The effective value of $\alpha_{IP}(0)$ as a function of Q^2. The squares correspond to $\alpha_{IP}(0) = 1 + \lambda$ extracted from a fit $F_2 = cx^{-\lambda(Q^2)}$ to inclusive $F_2(x, Q^2)$ [4] data for $x < 0.01$. The filled circles are the values of $\alpha_{IP}(0)$ as obtained from the phenomenological Regge fit to the F_2^D data as described in the text. The triangle is the value of $\alpha_{IP}(0)$ which was already measured by H1 using 94' data [6]

tive gluon distribution and was used to investigate the QCD and Regge factorization properties of diffractive DIS.

In Fig. 4a) the diffractive dijet cross section as a function of $z_{IP}^{(jets)}$ is shown, where $z_{IP}^{(jets)} = \frac{Q^2+M_{12}^2}{Q^2+M_X^2}$ and M_{12}^2 is the squared dijet invariant mass. In loose terms, the $z_{IP}^{(jets)}$ observable measures the fraction of the total hadronic final state energy of the X system that is contained in the two jets. Diffractively scattered $q\bar{q}$ photon fluctuations satisfy $z_{IP} = 1$ at the parton level and can be smeared to $z_{IP}^{(jets)}$ values as low as 0.6 because of fragmentation and jet resolution effects. Even taking this smearing into account, the $z_{IP}^{(jets)}$ distribution obviously implies the dominance of $q\bar{q}g$ over $q\bar{q}$ scattering in the proton rest frame picture. The distribution can also be very well fitted using

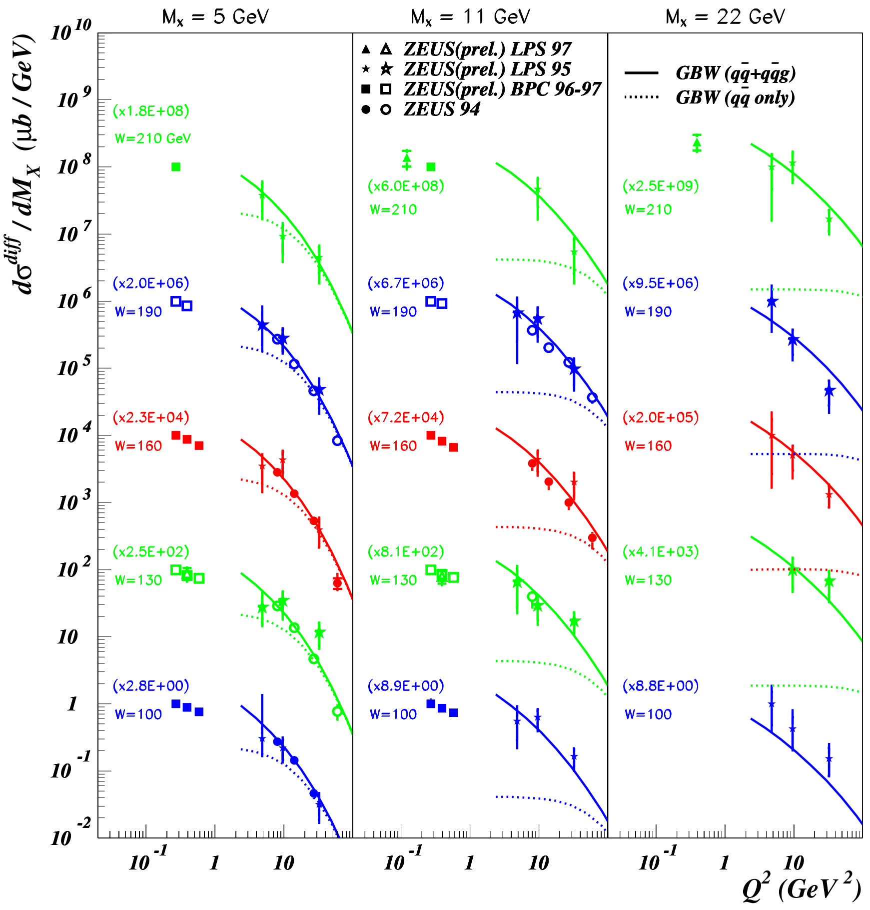

Figure 3. The diffractive cross sections for different W and M_X values as a function of Q^2 The continuous curves indicate the predictions of the model [7] for $q\bar{q}+q\bar{q}g$ fluctuations, the dashed ones are the predictions if only $q\bar{q}$ fluctuations are considered.

the parametrization based on the H1 leading order QCD fits to $F_2^{D(3)}$.

Making a fit to the shape of the $x_{I\!P}$ dependence of the cross section yields a value of $\alpha_{I\!P}(0) = 1.17 \pm 0.03(stat.) \pm 0.06(syst.)^{+0.03}_{-0.07}(model)$ for the Pomeron intercept, very close to the value measured using the $F_2^{D(3)}$ data.

The internal structure of the jets was studied in diffractive three-jet production in terms of differential jet shape [8], defined as the average of the fraction of the jet energy which lies inside an annulus of inner angular distance $\varphi - \delta\varphi$ and outer angular distance $\varphi + \delta\varphi$ from the jet axis. This is an interesting observable because gluon jets are known to be broader than quark jets. The differential jet shapes, $\rho(\varphi)$, were measured in the $\gamma^* I\!P$ center-of-mass frame, for the most-forward and most-backward jet in three-jet events, see

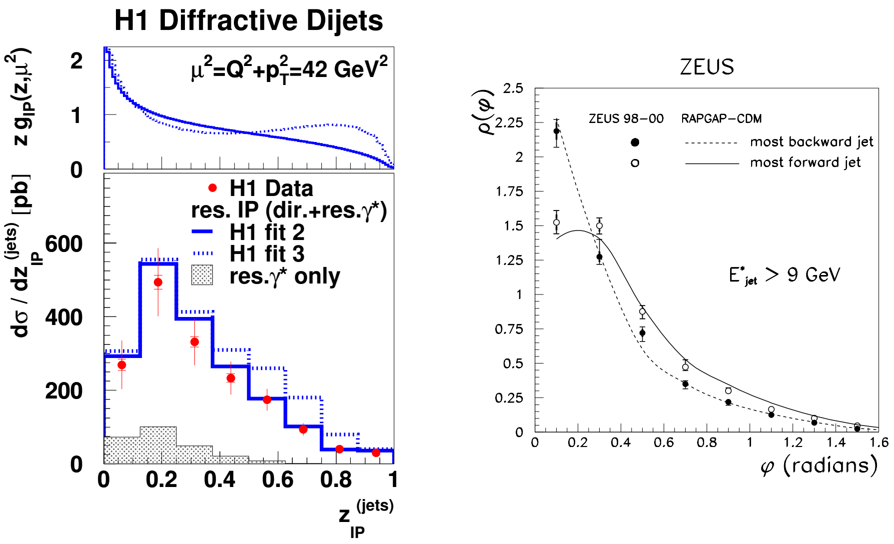

Figure 4. a) The diffractive dijet cross section as a function of $z_{IP}^{(jets)}$. The same data are compared to predictions of resolved pomeron models. The fits are based on the H1 leading order QCD fits to $F_2^{D(3)}$ [6]. b) The differential jet shape, $\rho(\varphi)$, for the most-forward and most-backward jets in three-jet events, where the Pomeron defines the forward direction.

Fig. 4b), where the forward region is defined by the IP direction. These measurements are described by models in which a gluon populates the Pomeron hemisphere and a quark is found in the photon direction, in good agreement with our knowlege about diffractive dynamics from the other inclusive measurements.

To summarize the *Inclusive* section, one can conclude that the data are broadly consistent with models in which the diffractive hadronic final-state is dominated by a $q\bar{q}g$ system with the gluon preferentially emitted in the Pomeron direction. Both the resolved Pomeron models with a pomeron, dominated by gluon, as well as the models where the virtual photon dissociates to a $q\bar{q}g$ system, which interacts with the proton via the exchange of a gluon ladder, provide a reasonable description of the measured distributions.

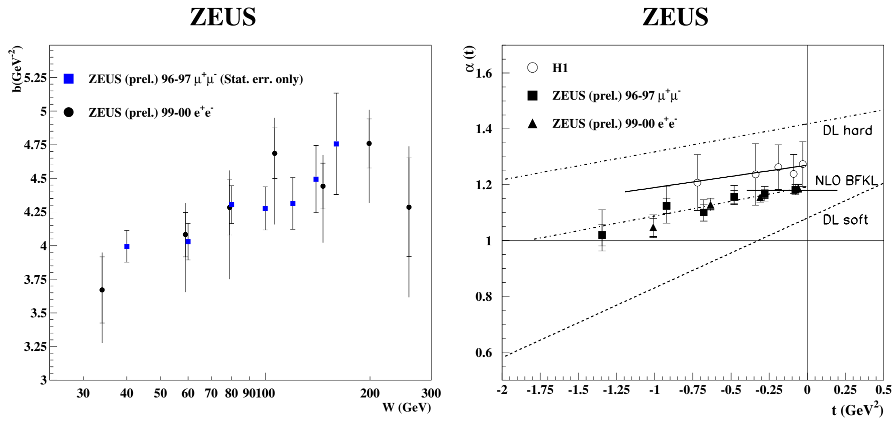

Figure 5. a) The b slope for the J/ψ photoproduction cross section versus W ; b) The Pomeron trajectory as a function of t from the H1 [10] and ZEUS experiments. The inner error bars indicate the statistical uncertainties errors, the outer bars are the statistical and systematic uncertainties added in quadrature. The result of straight line fits to the H1 and ZEUS data are shown. Also shown are the soft (dashed line) and the hard (dot-dashed line) DL Pomeron trajectories [11] and a prediction (shown by the solid line) for the Pomeron intercept based on a NLO BFKL calculation [12].

2.2 Exclusive diffraction

The exclusive, diffractive production of vector mesons, $ep \to eVp$, where $V = (\rho^0;\ \omega;\ \phi;\ J/\psi;\ \psi';\ \Upsilon)$ is measured at HERA in the region of $0 < Q^2 < 100$ GeV^2, $20 < W_{\gamma P} < 290$ GeV, $0 < |t| < 1.5$ GeV^2 and up to $|t| = 20$ GeV^2 for proton-dissociative events.

Photoproduction of J/ψ mesons ($Q^2 \approx 0$), contrary to the photoproduction of the light vector mesons, shows the signature of the perturbative regimes such as a steep rise of the total cross section with W, and can be described by perturbative QCD, since the mass of the charm quark provides a hard scale, similar to the Q^2 in the DIS case. At the same time, QCD models predict no variation of the t-dependence of the cross section with W.

Fitting the differential cross section as $\frac{d\sigma}{dt} \propto e^{-bt}$ the values of the slope b in different bins of W are obtained, see Fig. 5a). The data show the rise of the b slope with W, so called *shrinkage*, contrary to the pQCD expectation.

The photoproduction of J/ψ mesons can also be described within the framework of Regge phenomenology [9]. In this approach, $d\sigma/dt$ can be expressed at high energies as $\frac{d\sigma}{dt} \propto e^{bt} \cdot W^{2\cdot[2\alpha_{I\!P}-2]}$, where $\alpha_{I\!P}(t) = \alpha_{I\!P}(0) + \alpha'_{I\!P} t$

is the Pomeron trajectory. The W dependence of b can be used then to estimate $\alpha'_{I\!P}$, since $b = b_0 + 2\alpha'_{I\!P} ln(W/W_0)^2$. A fit to the data yields the $\alpha'_{I\!P} = 0.122 \pm 0.033(stat.) \pm^{+0.018}_{-0.032} (syst.)$ GeV^{-2}, that is much smaller than 0.25 of the *soft Pomeron*.

The Pomeron trajectory is also determined by measuring the variation of the energy dependence of the cross section at fixed t. The resulting values of $\alpha_{I\!P}(t)$ are presented in Fig. 5b) as a function of t and are fitted to the linear form yielding (the recent ZEUS data)

$\alpha_{I\!P}(0) = 1.201 \pm 0.013(stat.) \pm^{+0.003}_{-0.011} (syst.)$ and

$\alpha'_{I\!P} = 0.126 \pm 0.029(stat.) \pm^{+0.015}_{-0.028} (syst.)$ GeV^{-2}.

Analysis of the HERA vector meson cross-section ratios results shows that Q^2, M^2_{VM} and t can play a role of the hard scale in diffractive scattering [13,14]. The cross-section dependence is similar for Q^2 and M^2_{VM} and suggests using a combined scale $(Q^2 + M^2_{VM})$, but the t dependence is different. Existing pQCD models provide reasonable agreement with experimental data.

To summarize the *Exclusive* section, one can conclude that the data are consistent with the inclusive diffractive measurements, showing a larger value of the Pomeron intercept and a smaller value of the $\alpha'_{I\!P}$ in the presence of the hard scale.

References

1. ZEUS Coll. , M. Derrick et al. , Phys. Lett. **B 315**, 481 (1993)
2. H1 Coll. , T. Ahmed et al. , Nucl. Phys. **B 429**, 477 (1994)
3. See e.g. *Proc. of the Workshop on Future Physics at HERA*, G. Ingelman, A. DeRoeck and R. Klanner (eds.), Vol.2, DESY, Hamburg, (1996)
4. H1 Coll. , C. Adloff et al. , Eur. Phys. J. **C 21**, 33 (2001)
5. A. Donnachie and P.V. Landshoff, Phys. Lett. **B 296**, 227 (1992)
6. H1 Coll. , C. Adloff et al. , Z. Phys. **C 76**, 613 (1997)
7. K. Golec-Biernat and M. Wüsthoff, Phys. Rev. **D 60**, 114023 (1999)
8. ZEUS Coll. , S. Chekanov et al. , Phys. Lett. **B 516**, 273 (2001)
9. P.D.B. Collins, *An introduction to Regge Theory and Hogh Energy Physics*, Cambrige University Press, 1997
10. H1 Coll. , C. Adloff et al. , Phys. Lett. **B 483**, 23 (2000)
11. A. Donnachie and P.V. Landshoff, Phys. Lett. **B 470**, 243 (1999) and references therein.
12. S.J. Brodsky et al. , Sov. Phys. JETP **70**, 155 (1999)
13. H1 Coll. , C. Adloff et al. , Phys. Lett. **B-483**, 360 (2000)
14. ZEUS Coll. , S. Chekanov et al. , Abstr.556, *subm. to the EPS 2001, Budapest* 2001